Official journal of the American Society of Gene & Cell Therapy

MTOpen

original article

Kidney-specific Sonoporation-mediated Gene Transfer

Ryo Ishida[1], Daisuke Kami[2], Tetsuro Kusaba[1], Yuhei Kirita[1], Tsunao Kishida[3], Osam Mazda[3], Takaomi Adachi[1] and Satoshi Gojo[2]

[1]Division of Nephrology, Department of Internal Medicine, Graduate School of Medical Science Kyoto Prefectural University of Medicine, Kyoto Prefectural University of Medicine, Kyoto, Japan; [2]Department of Regenerative Medicine, Graduate School of Medical Science Kyoto Prefectural University of Medicine, Kyoto Prefectural University of Medicine, Kyoto, Japan; [3]Department of Immunology, Graduate School of Medical Science Kyoto Prefectural University of Medicine, Kyoto Prefectural University of Medicine, Kyoto, Japan

Sonoporation can deliver agents to target local organs by systemic administration, while decreasing the associated risk of adverse effects. Sonoporation has been used for a variety of materials and in a variety of organs. Herein, we demonstrated that local sonoporation to the kidney can offer highly efficient transfer of oligonucleotides, which were systemically administrated to the tubular epithelium with high specificity. Ultrasonic wave irradiation to the kidney collapsed the microbubbles and transiently affected the glomerular filtration barrier and increased glomerular permeability. Oligonucleotides were passed through the barrier all at once and were absorbed throughout the tubular epithelium. Tumor necrosis factor alpha (TNFα), which plays a central role in renal ischemia–reperfusion injury, was targeted using small interfering RNA (siRNA) with renal sonoporation in a murine model. The reduction of TNFα expression after single gene transfer significantly inhibited the expression of kidney injury markers, suggesting that systemic administration of siRNA under temporary and local sonoporation could be applicable in the clinical setting of ischemic acute kidney injury.

Received 25 May 2015; accepted 7 September 2015; advance online publication 27 October 2015. doi:10.1038/mt.2015.171

INTRODUCTION

Acute kidney injury (AKI) affects a growing number of hospitalized patients and raises clinical problems that are associated with high morbidity and mortality rates.[1–3] AKI has a number of etiologies that include interstitial nephritis, rapidly progressive glomerulonephritis, obstructive nephropathy, renovascular complications, sepsis, and toxic nephropathy but is frequently the consequence of ischemic insults.[4] Ischemic AKI is a frequent and serious complication for patients subjected to major cardiac, liver, vascular, or kidney surgery.[5] The renal ischemia–reperfusion injury (I/R) model in rodents has provided increased understanding of the mechanisms of ischemic AKI and improved treatment strategies.[6] Tumor necrosis factor alpha (TNFα) is thought to play an important role in the pathophysiology of renal I/R. Inhibition of TNFα ameliorated renal I/R and subsequent renal fibrosis.[7,8] These results suggest that anti-TNFα therapy could be a candidate against AKI. However, systemic administration of anti-TNFα agents to individuals with systemic inflammatory response syndrome, including AKI, increased the morbidity of infection and mortality,[9,10] suggesting that kidney-specific methods are required for ideal AKI treatment.

RNA interference (RNAi) is a biological process in which gene expression is silenced by sequence-specific small RNAs, including small interfering RNA (siRNA) and microRNA, through RNA degradation, translational inhibition, and histone methylation.[11] Since the effectiveness of RNAi in mammalian somatic cells was first reported in 2001,[12] the use of this technique has been broadly applicable for *in vivo* and *in vitro* genetic manipulations. Clinical trials have shown the effectiveness of siRNAs for the treatment of malignant tumors, including hepatic cancer[13] and ophthalmological diseases, such as neurovascular age-related macular degeneration[14] and diabetic macular edema,[15] suggesting that siRNAs are a useful class of therapeutic drugs. However, the anionic and hydrophilic properties of siRNA prevent it from being delivered into the cytosol, and siRNA stability in the blood is not high due to the presence of nucleases. Even after entering into the cytosol, off-target events and inflammatory reactions have to be overcome.[16]

To date, several gene delivery methods have been developed using recombinant viruses, chemical agents, and nano-sized particles.[17] Recently, ultrasound and microbubble ultrasound contrast agents have become increasingly popular for systemically targeting drugs and genes. Acoustic pressure emits jet and shock waves, causing the collapse of microbubbles that subsequently perturb cellular membranes and transiently disrupt vascular endothelial integrity. This increases the permeability of the targeted sites to circulating therapeutic agents.[18,19] This method, known as "sonoporation," can selectively deliver agents to organs and tissues of interest, even when therapeutic agents are administrated systemically. Lan *et al.*[20] first reported the inhibition of renal fibrosis by gene transfer of recombinant, inducible Smad7 using an ultrasound-microbubble system in a rat unilateral ureter obstruction model. Li *et al.*[21] also reported the sonoporation-enhanced transfer of recombinant adeno-associated virus into less permissive

Correspondence: Takaomi Adachi, Division of Nephrology, Department of Internal Medicine, Kyoto Prefectural University of Medicine; 465 Kajii cho, Kamigyo ku, Kyoto 602–8566, Japan. E-mail: taka117@koto.kpu-m.ac.jp and Satoshi Gojo, Department of Regenerative Medicine, Graduate School of Medical Science, Kyoto Prefectural University of Medicine, 465 Kajii cho, Kamigyo ku, Kyoto 602–8566, Japan. E-mail: gojos@koto.kpu-m.ac.jp

renal cell carcinoma. So far, the combination of sonoporation and oligonucleotides has never been examined for the kidney, which has a unique structure, a filtration barrier in Bowman's capsule with tubular epithelium to absorb the small molecules.

In this study, we found that sonoporation-mediated gene transfer (SMGT) to the kidney accelerated the permeability of the glomerular filtration barrier and enhanced the native, robust ability of the tubular epithelium to absorb small molecules. The renal SMGT provides high, efficient, specific oligonucleotide delivery to the kidney within less than 1 minute. Our finding that a single session of SMGT using siRNA against TNFα ameliorated the extent of kidney injury suggests that SMGT could reverse ischemic AKI.

RESULTS

Optimization of ultrasound conditions

We examined the relation between the sonoporation deliver setting and the degree of the kidney injury (**Supplementary Figure S1a**). We first set the output intensity to 2 W/cm^2 of output power for 1 minute of irradiation duration, according to previous reports.[22,23] Under this condition, expression of kidney injury molecule 1 (KIM1) did not increase as a result of ultrasound irradiation in immunostaining and western blotting, suggesting that ultrasound did not cause kidney injury (**Supplementary Figure S1b,c**). However, 2 minutes of exposure or 3 W/cm^2 intensity of the ultrasound caused significant kidney injury. From the safety aspect, we set the condition of the ultrasound as follows for subsequent studies: output intensity of 2 W/cm^2, duration time of 1 minute. In addition, we evaluated whether sonoporation caused fibrosis or inflammation at days 1, 3, 7, and 14 after sonoporation. Analysis of Masson's trichrome staining showed that sonoporation did not cause fibrosis at days 1, 3, 7, and 14 (**Supplementary Figure S1d**), and analysis of the macrophage staining (for F4/80) revealed that sonoporation did not cause macrophage infiltration at days 1, 3, 7, and 14 (**Supplementary Figure S1e**).

Localization of sonoporation-delivered oligonucleotides

To determine if we could efficiently deliver oligonucleotides into the kidney *in vivo* by sonoporation, we injected Dylight547-labeled oligonucleotides (DLO) alone or as a mixture with microbubble via the inferior vena cava (IVC) under laparotomy and exposed an ultrasonic wave directly to the kidney for 1 minute immediately after injection (**Figure 1b**). DLO was not detected in control animals that were subjected to ultrasound irradiation without injection. In ultrasound-irradiated animals injected with a mixture of DLO and microbubble, DLO was detected in proximal tubular epithelial cells and localized near the brush border. DLO was weakly detected in animals injected with DLO alone or in animals injected with a mixture of DLO and microbubble in the absence of ultrasound irradiation (**Figure 1c**). We did not detect DLO in other organs, such as brain, heart, lung, liver, spleen, testis, and gastrointestinal tracts, and we verified that the oligonucleotides were exclusively transferred into the targeted kidney for sonoporation (**Supplementary Figure S2**). The mRNA levels of KIM1 and neutrophil gelatinase-associated lipocalin (NGAL) did not increase as a result of this procedure (**Figure 1d,e**). These results indicate that an oligonucleotide was

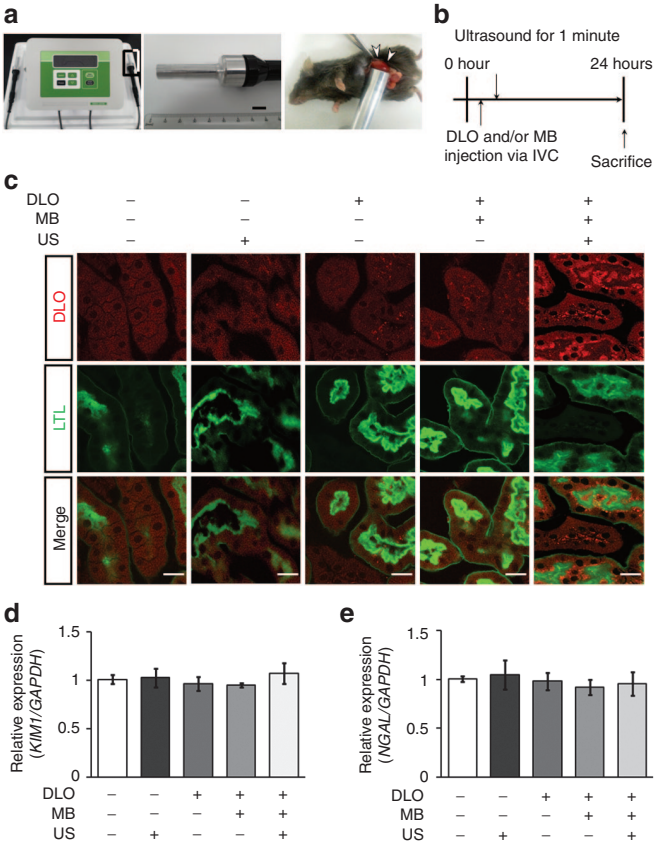

Figure 1 Dylight547-labeled oligonucleotides (DLO) were delivered into the kidney using sonoporation. (**a**) Sonitron 2000V (left) and its probe of 12 mm in diameter (middle). Bar = 10 mm. Ultrasound irradiation was performed on the left kidney (arrowhead) for 1 minute (right). (**b**) Experimental scheme. After median incisions, the mixtures of 1 nmol of DLO and microbubbles (MB) were injected via IVC using a syringe equipped with a 34-gauge needle. Immediately after injection, ultrasound irradiation was performed with an input frequency of 3 MHz, an output intensity of 2W/cm^2, and a pulse duty ratio of 50%, using Sonitron 2000V. The mice were sacrificed at day 1. (**c**) Distribution of DLO signals under different conditions of the intervention. DLO signal was detected more frequently in the animals injected with DLO and MB, with ultrasound irradiation, than in other animals. Co-staining with LTL showed DLO localization to nearby brush border in proximal tubular cells. Bar = 50 µm. (**d,e**) Relative expression of KIM1 and NGAL mRNAs. The result indicated that the kidney was not injured by DLO, MB, or ultrasound irradiation. Results are expressed as a ratio of the animals of DLO(-) MB(-) US(-) (n = 3). Data were expressed as mean ± SE. DLO, Dylight547-labeled oligonucleotides; IVC, inferior vena cava; LTL, Lotus tetragonolobus lectin; MB, microbubble; US, ultrasound irradiation.

delivered specifically into the kidney *in vivo* by sonoporation without causing kidney injury.

Immunofluorescence staining with Lotus tetragonolobus lectin showed that most of the DLO signal colocalized with Lotus tetragonolobus lectin immediately inside the brush border of tubular proximal epithelial cells, while immunofluorescence for Dolichos biflorus agglutinin showed that DLO signal was weakly detected in the collecting duct (**Figure 2**, upper two rows). In the glomerulus, DLO was weakly detected in endothelial cells, podocytes, and mesangial cells as indicated by immunofluorescence staining with CD31, podocin, and PDGFRβ, respectively (**Figure 2**, middle three rows). In the interstitium,

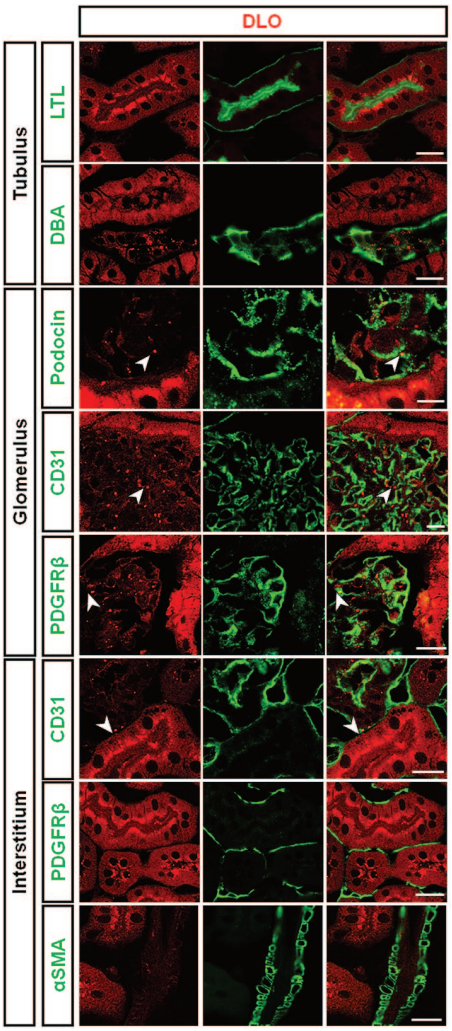

Figure 2 DLO was delivered mainly into proximal tubular cells. Upper two rows: Immunofluorescence staining with LTL shows that DLO was detected immediately inside the brush border of tubular proximal epithelial cells. Immunofluorescence staining with DBA shows that DLO was weakly detected in the collecting duct. Middle three rows: In the glomerulus, DLO was detected slightly in endothelial cells, podocytes, and mesangial cells as indicated by the immunofluorescence staining with CD31, podocin, and PDGFRβ, respectively. Lower three rows: In the interstitium, immunofluorescence staining with CD31 shows that DLO was slightly detected in endothelial cells. Bar = 10 μm. DBA, Dolichos biflorus agglutinin; DLO, Dylight547-labeled oligonucleotides; LTL, Lotus tetragonolobus lectin.

immunofluorescence staining with PDGFRβ, which is a marker for myofibroblasts, showed no colocalization with DLO. In the arteriole, αSMA, which is a marker for smooth muscle cells, did not colocalize with DLO (**Figure 2**, lower two rows).

Sonoporation transiently increases glomerular capillary permeability

To determine if glomerular capillary permeability is changed by sonoporation, we examined the fluorescence intensity of the urine that was collected after injection of the mixture of DLO and microbubble, with or without ultrasound irradiation (**Figure 3a**). We also examined the fluorescence intensity of the urine that was collected after the injection of DLO alone (**Figure 3a**). Before the

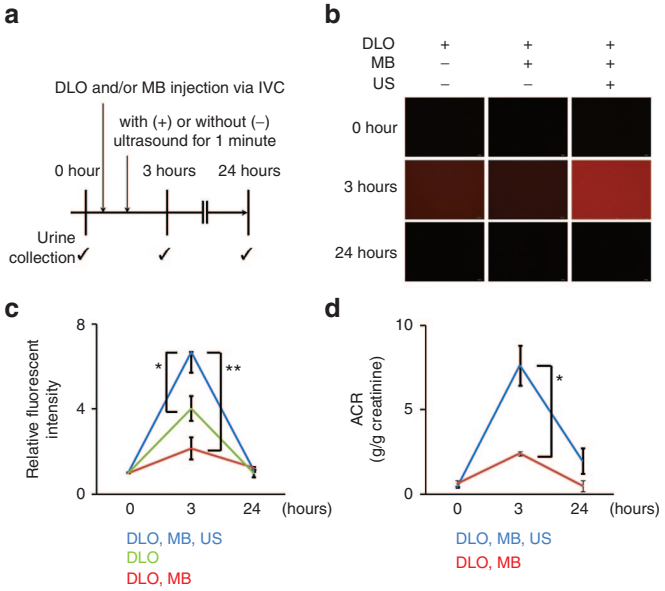

Figure 3 DLO into the urine was transiently increased by sonoporation. (**a**) Experimental scheme. After median incisions, 1 nmol of DLO with/without microbubbles (MB) were injected via IVC using a syringe equipped with a 34-gauge needle. Immediately after injection, ultrasound irradiation was performed. The urine was collected at 0, 3, and 24 hours after injection. (**b,c**) Fluorescence intensity of the urine. Fluorescence intensity was assessed using fluorescent microscopy and a 96-well microplate reader. The urine showed significantly stronger fluorescence intensity in animals injected with a mixture of DLO and microbubble with ultrasound irradiation than that in other animals. Results are expressed as a ratio in comparison to the animals of DLO(+) MB(+) US(-) at 0 hour (*$P < 0.05$; **$P < 0.01$; $n = 3$). (**d**) Transient increase of the glomerular capillary permeability caused by sonoporation. We considered the urine albumin–creatinine ratio as a parameter for glomerular permeability. The urine albumin–creatinine ratio transiently increased and returned to the original state. Results are expressed as a ratio in comparison to the animals of DLO(+) MB(+) US(-) at 0 hour (*$P < 0.05$; $n = 3$). Data were expressed as mean ± SE. ACR, albumin–creatinine ratio; DLO, Dylight547-labeled oligonucleotides; IVC, inferior vena cava; MB, microbubble; US, ultrasound irradiation.

injection, the urine was not fluorescent in any of the animals. After 3 hours of the injection, the urine was highly fluorescent in animals injected with a mixture of DLO and microbubbles, with ultrasound irradiation, while the urine was only weakly fluorescent in animals injected with a mixture of DLO and microbubbles, without ultrasound irradiation. The fluorescence intensity of urine showed from animals injected with DLO alone was significantly weaker than the intensity of urine from animals injected with both DLO and microbubble, with ultrasound irradiation, and there was no statistically significant difference between the animals injected with DLO alone and those injected with both DLO and microbubbles about the fluorescent intensity of the urine. After 24 hours of the injection, the urine was no longer fluorescent in any groups (**Figure 3b,c**). The microbubbles were not detected in the urine, which suggests that the microbubbles did not pass through the glomerular membrane (**Supplementary Figure S3**).

To determine if the sonoporation-induced increase in permeability of the glomerular capillary was transient, we measured the urine albumin–creatinine ratio (**Figure 3d**). The urine albumin–creatinine ratio also transiently increased at 3 hours after sonoporation and returned to the original state 24 hours after

sonoporation, suggesting that the glomerular capillary permeability returned to the original state.

Functionality of sonoporation transferred siRNA

Mice expressing green fluorescent protein (GFP) received a single dose of siRNA against GFP by renal SMGT, and the mRNA level of GFP was examined 1 day after sonoporation (**Figure 4a**). Quantitative reverse transcription polymerase chain reaction (qRT-PCR) indicated that the mRNA level of GFP in the kidney after sonoporation decreased to ~0.87-fold more than the GFP mRNA level in the contralateral kidney without sonoporation (**Figure 4b**). The mRNA level of GFP was not affected in other organs. As evaluated by fluorescent microscopy, there was no significant difference in the GFP protein expression level between that of the siGFP-injected animals with sonoporation and that of the other groups (**Supplementary Figure S4**).

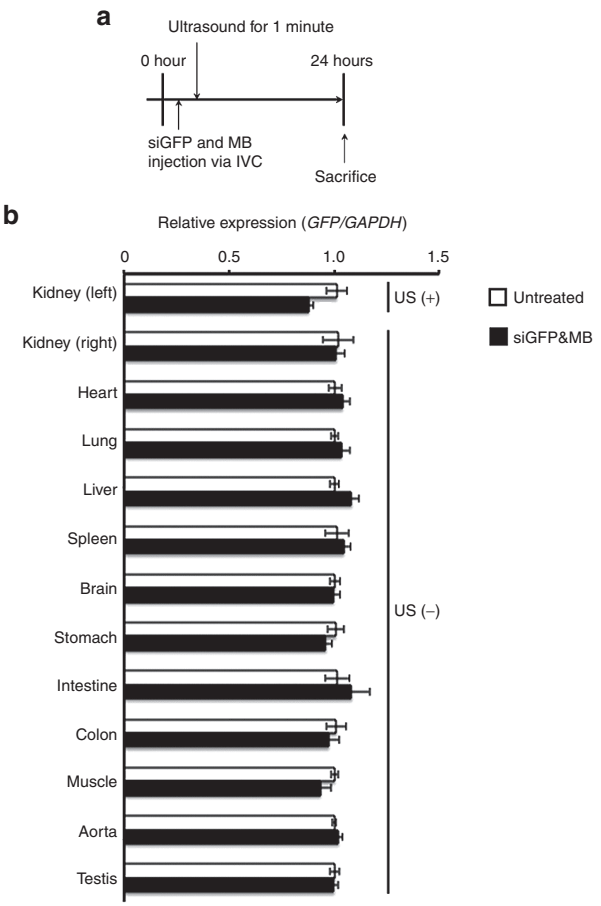

Figure 4 siRNA against GFP (siGFP) was delivered into the kidney using sonoporation. (**a**) Experimental scheme. After median incisions, the mixtures of 1 nmol of siGFP and microbubbles were injected via IVC using a syringe equipped with a 34-gauge needle. Immediately after injection, ultrasound irradiation was performed. The mice were sacrificed at day 1. (**b**) Relative expression of GFP mRNA in various organs. The expression level of GFP mRNA in the kidney in which sonoporation was performed significantly decreased in comparison to the expression in the contralateral kidney and other organs. Results are expressed as a ratio of the sham kidney (*$P < 0.05$; $n = 3$). Data were expressed as mean ± SE. IVC, inferior vena cava; siGFP & MB, mice injected with siRNA against GFP and microbubble; Untreated, untreated mice; US, ultrasound irradiation.

Delivery of oligonucleotides into injured kidney

After 30 minutes of bilateral renal I/R, we injected a mixture of DLO and microbubble via IVC and immediately exposed the left kidney to ultrasonic wave for 1 minute (**Figure 5a**). KIM1 and NGAL mRNA levels were significantly increased by the bilateral renal I/R, verifying that the procedure can be used to model kidney injury (**Figure 5b,c**). Neither injection of DLO nor sonoporation caused additional elevation of the mRNA levels of KIM1 and NGAL (**Figure 5b,c**). Co-staining of KIM1 and DLO showed that sonoporation allowed the transfer of oligonucleotides to the damaged epithelial cells (**Figure 5d**).

Delivery of siRNA against TNFα *in vitro*

We used siRNA against TNFα (siTNFα) using NIH3T3 cells to determine if siTNFα suppresses TNFα expression. First, we determined the suitable concentration of lipopolysaccharide (LPS) needed to increase TNFα mRNA expression in NIH3T3 cells by measuring cell number, cell viability, and TNFα mRNA level of NIH3T3 cells under different concentrations of LPS stimulation.[24] Cell number decreased in the presence of LPS and reached a plateau at a concentration of 1 μg/ml (**Supplementary Figure S6a**). Cell viability depended on the concentration of LPS (**Supplementary Figure S6b**). TNFα mRNA level increased approximately twofold at the concentration of 1 μg/ml; therefore, we used this concentration for subsequent experiments (**Supplementary Figure S6c**). We found that cell number and cell viability of NIH3T3 cells improved significantly (**Supplementary Figure S6d,e**) and that the level of TNFα mRNA decreased by ~0.5-fold upon treatment with siTNFα (**Supplementary Figure S6f**).

Delivery of siTNFα by sonoporation *in vivo*

We determined if siTNFα was delivered by sonoporation into the injured kidney, and we also evaluated any subsequent function. After the right nephrectomy and 30 minutes of unilateral I/R on the left kidney, we injected a mixture of siTNFα and microbubble via IVC and immediately exposed the left kidney to ultrasonic wave for 1 minute (**Figure 6a**). The mRNA level of TNFα significantly increased in animals subjected to 30 minutes of unilateral I/R when compared to the TNFα mRNA level of sham-treated animals (**Figure 6b**). The mRNA level of TNFα was not impacted by either the injection of siTNFα alone nor sonoporation alone. The mRNA level of TNFα decreased ~0.5-fold upon single injection of siTNFα with sonoporation (**Figure 6b**). These results indicated that we could prevent the elevation of TNFα mRNA caused by renal I/R by sonoporation into the targeted kidney. The mRNA levels of KIM1 decreased significantly in the animals injected with siTNFα with sonoporation (**Figure 6c**). The mRNA levels of NGAL tended to decrease in animals injected with siTNFα with sonoporation (**Figure 6d**). The immunofluorescent staining and western blotting of KIM1 shows that KIM1 protein also decreased in siTNFα-injected animals with sonoporation (**Figure 6e,f**). In the analysis of the inflammatory cytokines, the mRNA levels of TGFβ and IL1β significantly decreased in siTNFα-injected animals with sonoporation (**Figure 7**). The mRNA levels of IL1α, MIP2, and MCP1 also tended to decrease with sonoporation in siTNFα-injected animals (**Figure 7**). There was no statistically significant difference between the group of siTNFα-injected animals with sonoporation and the

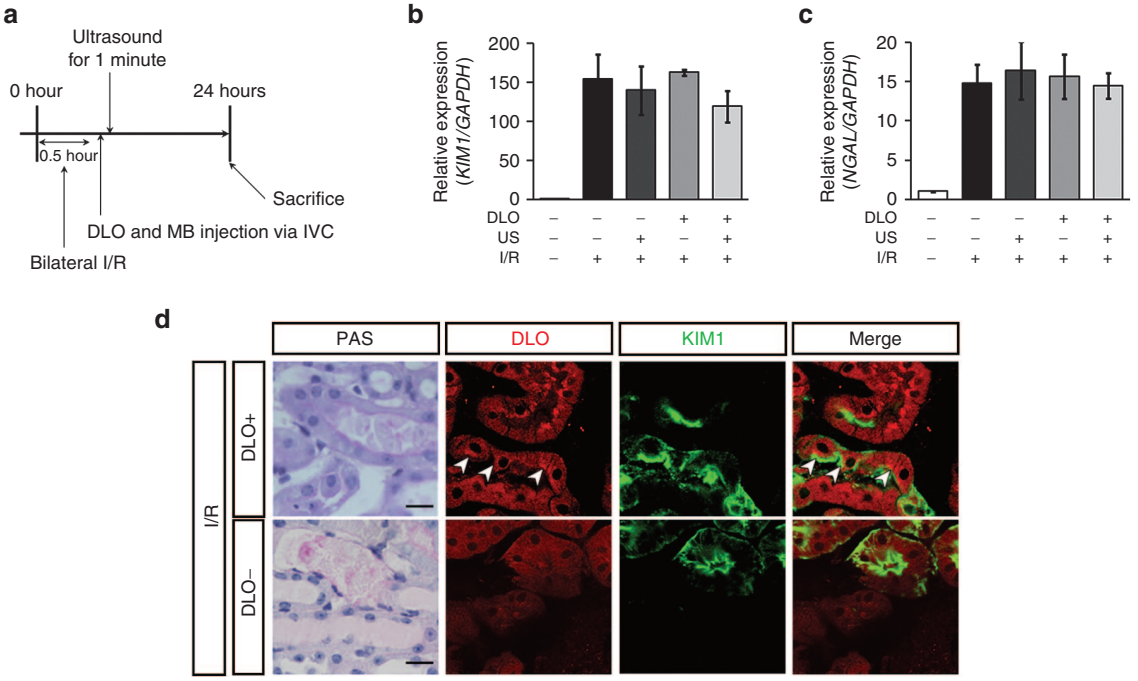

Figure 5 DLO was delivered into the injured epithelial cells. (**a**) Experimental scheme. After median incisions and 30-minute bilateral I/R, a mixture of 1 nmol of DLO and microbubbles were injected via IVC using a syringe equipped with a 34-gauge needle. Immediately after injection, sonoporation was performed on the left kidney. The mice were sacrificed at day 1. (**b, c**) Relative expression of KIM1 and NGAL mRNAs. KIM1 and NGAL mRNA levels increased in renal I/R animals. Neither injection of DLO nor sonoporation caused additional elevation of KIM1 and NGAL mRNAs. Results are expressed as a ratio of the sham (n = 3). Data were expressed as mean ± SE. Sham means DLO(-) US(-) I/R(-). (**d**) Co-immunofluorescence staining with KIM1 and DLO. DLO signal was detected in the KIM1-positive injured epithelial cells (upper row). Bar = 50 µm. DLO, Dylight547-labeled oligonucleotides; I/R, ischemia-reperfusion. IVC, inferior vena cava; US, ultrasound irradiation.

other groups in histological damage and serological renal function, evaluated by injury score and serum blood urea nitrogen, respectively (**Supplementary Figure S5a,b**).

DISCUSSION

This study demonstrates that sonoporation can effectively and selectively deliver oligonucleotides into the kidney without adverse effects through a mechanism that involves transient acceleration of the permeability of glomerular filtration barriers. Murine I/R kidney can be ameliorated by introducing siRNA against TNFα with sonoporation.

Many gene transfer modalities, such as recombinant viruses and chemical materials, have been developed to be applied in basic science and gene therapy.[17] However, genetic modifications using recombinant viruses still raise concerns about safety. Because of its safety profile, siRNA is expected to be the next-generation method of choice for gene therapy.[25] There have been previous reports of siRNA transfer into the kidney,[26] including siRNA delivery into the glomeruli[27,28] and the tubules[29–31] using techniques such as hydrodynamics, electroporation, nanocarrier complexation, and the antibody-delivery system in which antipodocyte antibodies are modified by the cleavage of divalent immunoglobulin G and positive charging to allow carrying of negatively charged siRNA that specifically binds to the podocytes, followed by internalization and transportation to the cytoplasm.[32] In order to use siRNAs as therapeutic agents in various applications, the instability and the difficulty of passage through the cell membrane due to the hydrophilic properties of siRNA[33] should be resolved, and sonoporation can be used to overcome these problems. Sonoporation has been reported to deliver genes directly to target organs and can result in high levels of gene expression without harming the target organs.[34]

In this study, we demonstrated the ability to deliver oligonucleotides by sonoporation specifically into the kidney. Kurosaki *et al.*[23] previously demonstrated that plasmid DNA containing the luciferase gene could be delivered by sonoporation specifically into the kidney by measuring the level of luciferase gene expression. Lan *et al.*[20] also reported that the combination of ultrasound and microbubbles largely enhances plasmid DNA transfer into the kidney, resulting in more than a 1,000-fold increase in the transfection rate, compared to the non-ultrasound treatment. Immunofluorescence co-staining suggested that DLO accumulation is more frequent in the proximal tubules than in other compartments in the kidney,[23] which was consistent with our results. We also demonstrated that the distribution of DLO in the injured kidney is similar to the distribution in normal kidney, suggesting that oligonucleotides could be delivered into the proximal tubules by sonoporation even during ischemic AKI. These results support the use of SMGT for clinical treatment of ischemic AKI, because cells targeted by ischemic insult are mainly the proximal tubular epithelial cells.[35]

Two previous reports about SMGT to the kidney did not determine the mechanism of gene transfer.[20,23] We found that the sonoporation phenomenon occurs at the glomerular filtration barriers and that gene transfer takes advantage of the native absorbable capability of the tubular epithelium. Our results indicated that the

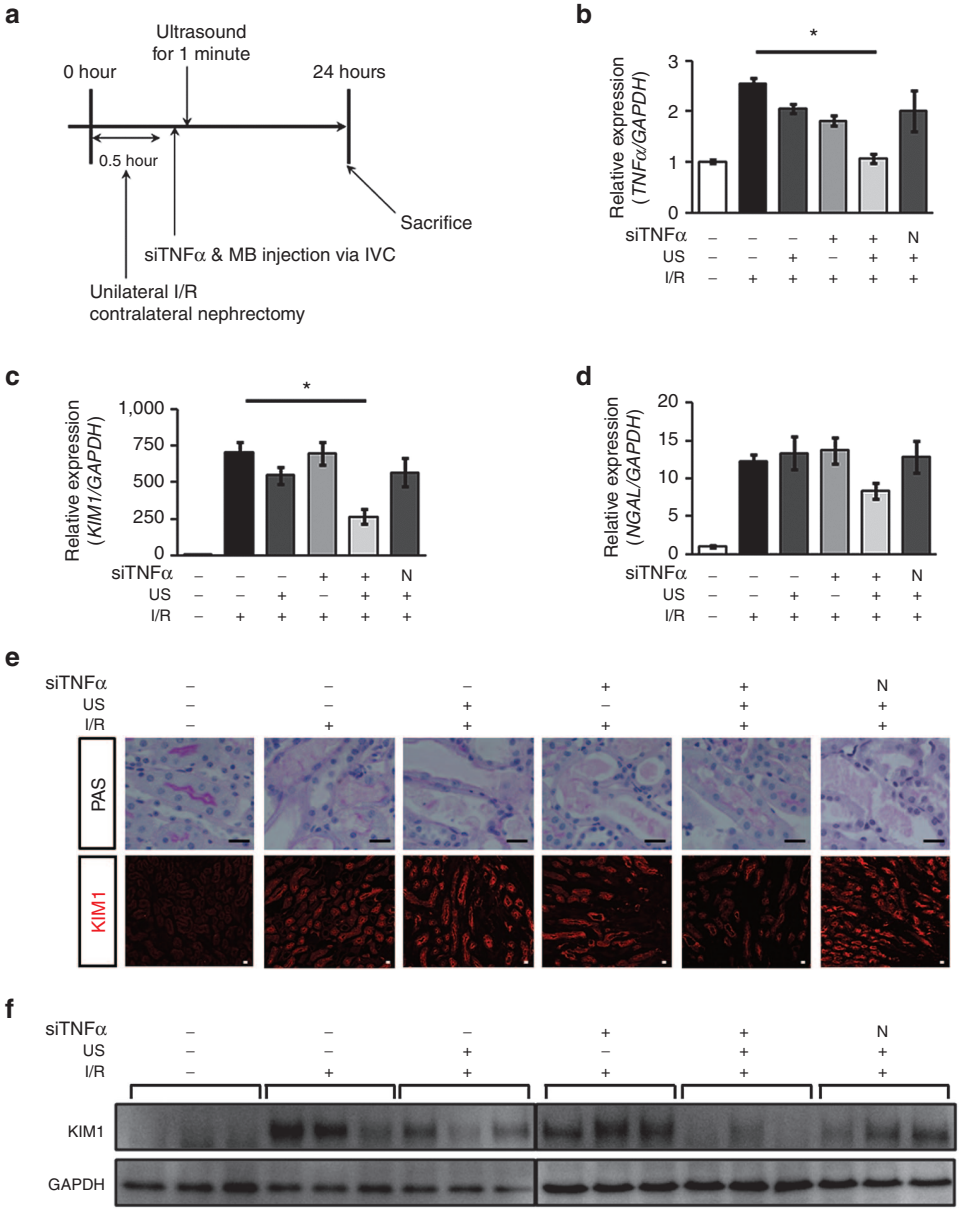

Figure 6 Kidney injury significantly improved in animals injected with siTNFα with sonoporation in renal IRI model. (**a**) Experimental scheme. After median incisions, 30-min unilateral I/R, and right nephrectomy, the mixture of 1 nmol of siTNFα and microbubbles were injected via IVC using a syringe equipped with a 34-gauge needle. Immediately after injection, ultrasound irradiation was performed. The mice were sacrificed at day 1. (**b–d**) Relative expression of TNFα, KIM1, and NGAL mRNAs. The mRNA expression level of TNFα and KIM1 significantly decreased in animals injected with siTNFα with sonoporation compared to the expression in untreated I/R animals. The mRNA levels of NGAL tended to decrease with injection of siTNFα with sonoporation compared to the levels in other animals. Results of relative expression of mRNAs are expressed as a ratio of the sham (*$P < 0.05$; $n = 10$). Data were expressed as mean ± SE. (**e**) Periodic acid–Schiff (PAS) staining (upper row) and immunofluorescence staining with KIM1 (lower row). KIM1 was detected in proximal tubular epithelial cells in the IRI groups, and the strength of the fluorescence decreased in animals injected with siTNFα with sonoporation. (**f**) Western blot analysis of KIM1 and GAPDH was used as an internal control. KIM1 protein decreased in animals injected with siTNFα with sonoporation. Bar = 50 μm. I/R, ischemia–reperfusion; IVC, inferior vena cava; N, negative control siRNA; NGAL, neutrophil gelatinase-associated lipocalin; siTNFα, kidney injected with siRNA against TNFα and microbubble; US, ultrasound irradiation.

urine was highly fluorescent in animals injected with a mixture of DLO and microbubble, with ultrasound irradiation, suggesting that the oligonucleotides were simultaneously passed through the glomerular filtrate by sonoporation. Although it is known that naked siRNA is gradually filtered into the urine,[36,37] it is thoroughly and promptly removed into the proximal tubules at the time of the insonation. High concentrations of siRNA at times may lead to siRNA distribution throughout the tubular epithelium. Because microbubble was not observed in the bladder following ultrasonic wave irradiation, sonoporation likely does not contribute to reabsorption from the apical side of the epithelial cells. We also detected DLO immediately inside the brush border of tubular proximal epithelial cells, suggesting that the oligonucleotides are delivered from the apical side, because the distribution of DLO accumulation in the proximal tubules is similar to the distribution of reabsorbed labeled albumin.[38]

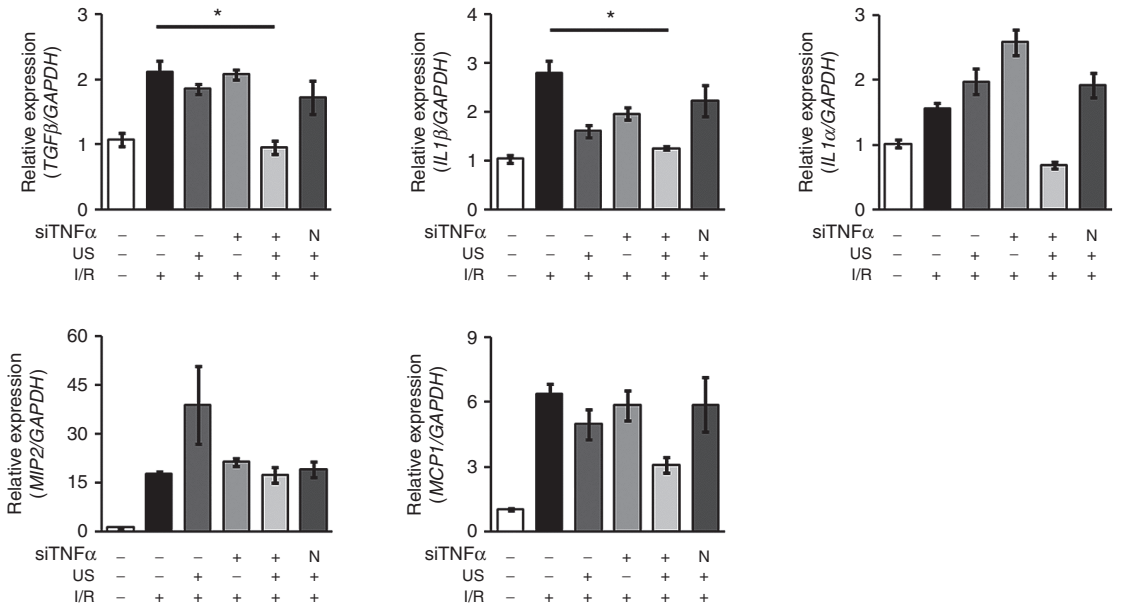

Figure 7 The analysis of the inflammatory cytokines. The mRNA level of TGFβ and IL1β significantly decreased in animals injected with siTNFα, with sonoporation. The mRNA levels of IL1α, MIP2, and MCP1 also decreased in animals injected with siTNFα with sonoporation. Results of relative expression of mRNAs are expressed as a ratio of the sham (*P < 0.05; n = 10). Data were expressed as mean ± SE. I/R, ischemia-reperfusion; N, negative control siRNA; siTNFα, kidney injected with siRNA against TNFα and microbubble; US, ultrasound irradiation.

When SMGT is applied during clinical treatment, safety is most important. Because the ultrasonic wave is absorbed in the tissues of the organ and turns into thermal energy, too much exposure can cause an increase in organ temperature and cause organ damage. In this study, we adjusted the strength and duration of treatment to find an adequate condition that would efficiently transfer the genes without causing damage to the kidney. This step is consistent with a previous study using SMGT to the kidney.[23] The kidney injury was determined by histopathological assessment and by measuring the levels of KIM1 and NGAL mRNA in the kidney, which are sensitive biomarkers for kidney injury.[39,40] The results suggest that sonoporation causes little renal damage if the strength of the ultrasound and the duration of the treatment are adjusted. We also showed that the sonoporation-induced increase in the glomerular capillary permeability is transient. This result indicated that sonoporation did not harm the kidney in spite of the continuous proteinuria associated with the increase in the glomerular capillary permeability, which might result in the chronic kidney damage.[41]

Previous reports demonstrated siRNA delivery to the targeted tissues and organs by sonoporation. Tsunoda *et al.*[42] reported that the GFP expression level of the coronary artery wall in enhanced GFP-transgenic mice was reduced by sonoporation-delivered siGFP. Un *et al.*[43] reported that siRNA against intracellular adhesion molecule-1 (ICAM-1), delivered by sonoporation specifically into the hepatic endothelial cells, suppressed ICAM-1 expression in different models of acute liver inflammation. Moreover, Inoue *et al.*[22] reported that siTNFα injected into the articular joints was delivered into the synovial tissue by sonoporation and decreased the level of TNFα, resulting in the amelioration of the radiographic score upon histological examination. In the field of the nephrology, our study is the first to report that siRNA could be delivered specifically into the targeted kidney by sonoporation and to confirm the function of the delivered siRNA.

Increasing evidence has implicated TNFα as a major participant in the pathogenesis of kidney injury, promoting inflammation, apoptosis, and accumulation of extracellular matrix.[43–45] The pathogenic role of TNFα and the potential benefits of modulating TNFα activity have been shown in models of various kidney diseases, including AKI.[7,44–46] However, previous reports showed that systemic administration of anti-TNFα agents increased the opportunity of infection,[9,10] suggesting that kidney-specific treatment is required to reduce the side effect of the agent. We designed kidney-specific gene transfer for silencing TNFα to repress AKI. The repression of TNFα suppressed KIM1 expression, which has been shown to improve ischemic AKI. Our intervention showed a crucial effect against AKI. The repression of TNFα might stop the vicious cycle of ischemic AKI, although ischemic AKI is attributed to many factors, including other inflammatory cytokines,[47–49] intracellular apoptotic regulation molecules,[50,51] cell adhesion molecules,[52,53] and infiltrating immune cells.[54–56] Microbubbles have previously been reported to be retained within the microcirculation of inflamed tissue.[57,58] Inflammatory processes are involved in the pathogenesis of AKI, so the ability of microbubbles to accumulate in inflamed tissues might lead to an increased opportunity for the simultaneous existence of microbubbles and siRNA in an I/R model. We suggest that anti-TNFα therapy, using siRNA delivered by sonoporation, could be an effective therapy against ischemic AKI.

The limitation of this study lies in the difficulty of translating the method for clinical use. The application of ultrasound irradiation directly to the kidney and siRNA injection via the IVC would be too invasive as a clinical therapy. However, if our method was applied in human AKI therapy, percutaneous ultrasound irradiation and siRNA injection via a cutaneous vein could be performed as less-invasive methods. Further research is required to develop an adequate method of ultrasound irradiation and siRNA

injection for clinical application. In addition, the adjustment of the dose and the frequency of siRNA injection for human AKI could contribute to improvement of the condition.

In conclusion, we showed that we could deliver siRNA into the kidney specifically and effectively using sonoporation through transient acceleration of the permeability of the glomerular filtration barriers. We also showed that systemic administration of TNFα siRNA under temporary and local sonopration could ameliorate ischemic AKI. We suggest that our intervention would be a strong candidate of the therapy to overcome AKI.

MATERIALS AND METHODS

Animal treatment. C57BL/6 male mice and GFP mice,[59] aged 10 weeks and weighing 23–28 g, were used. Mice were housed under a 12/12-hour day/night cycle with free access to food and water. All studies were approved by the Committee for Animal Research, Kyoto Prefectural University of Medicine.

The ischemia/reperfusion model mice were anesthetized with an i.p. injection of 50 mg/kg pentobarbital sodium and placed on a homeothermic table to maintain body temperature at 37 °C during surgery. Median incisions were made to expose renal pedicles. After the right nephrectomy, the left renal pedicle was clamped unilaterally with an arterial microclamp and released after 30 minutes. Reperfusion was confirmed visually, and the wounds were sutured. After surgery, mice had free access to water and chow. Kidneys were collected at 1 day after I/R. Sham control animals were subjected to identical surgery except for left renal pedicle clamping.

***Sonoporation-assisted oligonucleotide transfection* in vivo.** The mice were anesthetized, and I/R was performed. Aliquots of 100 µl of SV-25 microbubbles (NepaGene, Chiba, Japan) were added to 1 nmol of siRNA, and the mixtures were injected via IVC using a syringe equipped with a 34-gauge needle (React System, Osaka, Japan). Immediately after injection, a collimated ultrasound beam was applied for 1 minute through a probe 12 mm in diameter with an input frequency of 3 MHz, an output intensity of 2 W/cm^2 (spatial average temporary peak), and a pulse duty ratio of 50%, using a Sonitron 2000 V (serial no. 0624081173; NepaGene). The oligonucleotides that we used were as follows: miRIDIAN microRNA Mimic Transfection Control with Dy547 (Dylight547) was purchased from GE Healthcare (Little Chalfont, UK) and Silencer Select siRNA against GFP (siGFP), TNFα (siTNFα), and negative control siRNA were purchased from Life Technologies (Carlsbad, CA).

Tissue preparation. Mice were anesthetized and sacrificed, immediately perfused with phosphate-buffered saline from the left ventricle, and their kidneys were harvested. For frozen sections, kidneys were fixed with 4% paraformaldehyde for 2 hours on ice, incubated in 30% (v/v) sucrose at 4 °C overnight, and embedded in optimum cutting temperature compound (Sakura Finetek Japan, Tokyo, Japan). Frozen tissues were sectioned at 8 µm. For paraffin sections, kidneys were fixed with 4% (v/v) formalin and paraffin embedded, and paraffin-embedded tissues were sectioned at 4 µm.

Histological analysis. Renal morphology was observed in 8-µm paraffin sections along the long axis at the center of the kidney by Periodic acid–Schiff staining (Sigma-Aldrich, St Louis, MO). The histological changes that were evaluated included the percentage of renal tubules that displayed cell lysis, loss of brush border, and cell detachment. The development of tissue damage (referred to as kidney injury score) was scored as follows: 0, 0–25%; 1, 25–50%; 2, 50–75%; and 3, 75–100%. Ten nonoverlapping fields in the corticomedullary region (magnification: ×200) per kidney were randomly selected in a blinded manner and examined.

Immunohistochemistry and antibodies. Immunohistochemical staining to detect macrophages was performed using rat antimouse F4/80 antibodies (Serotec, Oxford, UK). Macrophages were counted in the corticomedullary region in 10 randomly chosen, nonoverlapping high-power fields (magnification: ×200).

Fibrosis analysis. The fibrosis area was counted in 10 randomly chosen, nonoverlapping high-power fields (magnification: ×200) using ImageJ software, based on Masson's trichrome staining.

Immunofluorescence analysis and antibodies. Samples were blocked with 5% (v/v) normal goat serum in phosphate-buffered saline and incubated with primary antibodies including fluorescein isothiocyanate (FITC)–conjugated anti-Lotus tetragonolobus lectin (FL-1321; Vector Laboratories, Burlingame, CA), FITC-conjugated anti-Dolichos biflorus agglutinin (FL-1031; Vector Laboratories), FITC-conjugated anti-CD31 (RM5201; Life Technologies), FITC-conjugated antipodocin (bs-6597R-FITC; Bioss, Woburn, MA), FITC-conjugated anti-PDGFRβ (sc-432 FITC; Santa Cruz Biotechnology, Santa Cruz, CA), and goat anti–KIM-1 (AF1817; R&D Systems, Minneapolis, MN). Secondary antibodies were either Alexa Fluor 488–conjugated antigoat immunoglobulin G (A-11078, Life Technologies) or Alexa Fluor 555–conjugated antigoat immunoglobulin G (A-21432; Life Technologies). Samples were incubated with secondary antibodies for 1 hour. Nuclear counterstaining was performed using 4′,6-diamidino-2-phenylindole and followed by mounting in Prolong-Gold (Thermo Fisher Scientific, Waltham, MA). Images were obtained by confocal microscopy (Nikon C1 Eclipse; Nikon, Tokyo, Japan) or standard microscopy (Nikon Eclipse 90i; Nikon). In GFP protein expression, whole kidney was observed by Fluorescent Stereo Microscope named fluorescent in vivo imaging system (KURAVIC-vivo; KURABO, Osaka, Japan).

Assessment of renal function. The blood samples were collected and clotted at room temperature. The samples were centrifuged at 8,000 × *g* for 5 minutes, and then, the supernatants were collected as serum. The blood urea nitrogen level was examined by LSI Medience (Tokyo, Japan).

RNA extraction and qRT-PCR. Total RNAs from cells were extracted using TRIzol (Life Technologies) and Direct-zol RNA MiniPrep Kit (Zymo Research, Irvine, CA) according to the manufacturer's recommendations. To perform qRT-PCR, 400 ng of total RNAs were reverse-transcribed using PrimeScript RT reagent Kit (Takara Bio, Shiga, Japan) and KAPA SYBR FAST qPCR Kit Master Mix (2×) Universal (KAPA BIOSYSTEMS, Boston, MA) according to the manufacturer's recommendations. qRT-PCR was performed using a Thermal Cycler Dice Real Time System (Takara Bio). All of the reactions were done in triplicate. The primers used in this experiment are listed in **Supplementary Table S1**.

Western blotting. Western blot analysis was used for detection of KIM1 expression within the kidney. Briefly, kidney tissues were lysed in sodium dodecyl sulfate sample buffer (0.5 mol/l Tris–HCl (pH 6.8), 10% sodium dodecyl sulfate 2% (w/v), glycerol 10% (v/v)). Samples were centrifuged at 12,000 × *g* for 10 minutes to pellet cell debris. Samples were mixed with bromophenol blue and 2-mercaptoethanol, boiled for 10 minutes, electrophoresed on a 10% sodium dodecyl sulfate polyacrylamide gel, and electroblotted onto a polyvinylidene difluoride transfer membrane (Millipore, Billerica, MA). The membrane was blocked in phosphate-buffered saline containing 3% bovine serum albumin, 0.05% Tween 20, and then incubated for 1 hour with goat monoclonal antibodies to KIM1 (AF1817; R&D Systems). After washing, the membrane was incubated with a 1:2,000 dilution of horseradish peroxidase–conjugated rabbit antigoat immunoglobulin G (sc-2922; Santa Cruz Biotechnology) in phosphate-buffered saline containing 3% bovine serum albumin. The blots were then developed using the ECL detection kit (Clarity Western ECL Substrate; Bio-Rad Laboratories, Richmond, CA), and protein bands were visualized using the VersaDoc system (Bio-Rad).

Measurement of glomerular capillary permeability. Mice were anesthetized and injected with mixtures of 100 µl of SV-25 microbubbles (NepaGene) and 1 nmol of DLO via IVC. Immediately after injection, a

collimated ultrasound beam was applied for 1 minute through a probe 12 mm in diameter with an input frequency of 3 MHz, an output intensity of 2 W/cm^2, and a pulse duty ratio of 50%, using a Sonitron 2000 V (serial no. 0624081173; NepaGene). Urine was collected before the injection, and then at 3 and 24 hours after injection. The fluorescence intensity of DLO in urine was evaluated using standard microscopy (Nikon Eclipse 90i) and a microplate reader (Infinite 200; Tecan, Männedorf, Switzerland). Urine albumin and creatinine were measured by Wako Pure Chemical Industries (Osaka, Japan).

Detection of the microbubbles in the urine. Mice were anesthetized and injected with mixtures of 100 µl of SV-25 microbubbles (NepaGene) via IVC. Immediately after injection, a collimated ultrasound beam was applied for 1 minute through a probe 12 mm in diameter with an input frequency of 3 MHz, an output intensity of 2 W/cm^2, and a pulse duty ratio of 50%, using a Sonitron 2000 V (NepaGene). Immediately after ultrasound irradiation, the bladder was observed by Vevo 2100 (Fujifilm VisualSonics, Toronto, Canada) to detect the microbubbles into the urine. The bladder was observed for 30 minutes after ultrasound irradiation.

***Cell line, culture, and treatment* in vitro.** NIH3T3 cells were cultured in Dulbecco's modified Eagle medium, 10% fetal bovine serum, and antibiotics (1% penicillin and streptomycin). We seeded 1×10^5 NIH3T3 cells per well in six-well plates (Thermo Fisher Scientific), cultured them for 24 hours, and treated them with different concentrations of LPS (0, 1, 2, 4, 8, and 16 µg/ml; *Escherichia coli* 0111:B4; Sigma-Aldrich; no. L4391) for 48 hours. The number and viability of cells was evaluated using a commercial, automatic, cell counting machine (ADAM-MC Automatic Cell Counter; NanoEnTek, Seoul, Korea) as described in previous studies.[60]

***Transfection of siRNA against TNFα* in vitro.** siTNFα was transfected into cultured NIH-3T3 cells that subsequently were onto six-well plates at a density of 1×10^5 cells/well. After 24 hours, cells were rinsed and supplemented with 2 ml of fresh culture medium. Nine microliters of Lipofectamine RNAiMAX Reagent was diluted into 150 µl of Opti-MEM medium (Life Technologies). siRNA at 400 ng was diluted into 150 µl of Opti-MEM medium. Therefore, diluted siRNA was added to diluted Lipofectamine RNAiMAX Reagent (1:1 ratio) and incubated for 5 minutes at room temperature. After incubating cells with the mixture for 1 day at 37 °C, we analyzed transfected cells.

Statistical analysis. Results are expressed as mean ± SE. Each experiment was performed using at least three mice per group and repeated in its entirety at least once with similar results. The quantification was performed from at least 10 high-power field pictures for each kidney. Statistical analysis was performed using the unpaired *t*-test. Multiple group comparisons were performed using one-way analysis of variance with a *post hoc* Tukey–Kramer test. $P < 0.05$ was considered statistically significant. Statistical analysis was performed using Excel 2007 (Microsoft, Redmond, WA), with the Statcel2 plug-in software (OMS Publishing, Saitama, Japan).

SUPPLEMENTARY MATERIAL

Figure S1. Ultrasound irradiation was performed using the Sonitron 2000 V with an input frequency of 3 MHz and a pulse duty ratio of 50%.

Figure S2. Distribution of DLO in other organs.

Figure S3. Detection of microbubbles in urine.

Figure S4. GFP protein expression observed by fluorescent in vivo imaging system (KURABO KURAVIC-vivo) (upper row) and microscopy (lower row).

Figure S5. Histological and serological analysis of the treated kidney.

Figure S6. Confirmation of siTNFα activity using NIH3T3 cells with lipopolysaccharide (LPS) treatment.

Table S1. Primer sets for quantitative RT-PCR.

ACKNOWLEDGMENTS

We express our sincere thanks to Hiroaki Inoue and Yuji Arai (Department of Orthopaedics, Kyoto Prefectural University of Medicine, Kyoto, Japan) for their guidance in the utilization of Sonitron 2000V. This research was supported by grants from the Ministry of Education, Culture, Sports, Science and Technology of Japan. The authors declare that there are no competing interests.

REFERENCES

1. Rewa, O and Bagshaw, SM (2014). Acute kidney injury-epidemiology, outcomes and economics. *Nat Rev Nephrol* **10**: 193–207.
2. Xue, JL, Daniels, F, Star, RA, Kimmel, PL, Eggers, PW, Molitoris, BA *et al.* (2006). Incidence and mortality of acute renal failure in Medicare beneficiaries, 1992 to 2001. *J Am Soc Nephrol* **17**: 1135–1142.
3. Lafrance, JP and Miller, DR (2010). Acute kidney injury associates with increased long-term mortality. *J Am Soc Nephrol* **21**: 345–352.
4. Tögel, F and Westenfelder, C (2014). Recent advances in the understanding of acute kidney injury. *F1000Prime Rep* **6**: 83.
5. Elapavaluru, S and Kellum, JA (2007). Why do patients die of acute kidney injury? *Acta Clin Belg Suppl* 326–331.
6. Bonventre, JV and Weinberg, JM (2003). Recent advances in the pathophysiology of ischemic acute renal failure. *J Am Soc Nephrol* **14**: 2199–2210.
7. Daemen, MA, van de Ven, MW, Heineman, E and Buurman, WA (1999). Involvement of endogenous interleukin-10 and tumor necrosis factor-alpha in renal ischemia-reperfusion injury. *Transplantation* **67**: 792–800.
8. Adachi, T, Sugiyama, N, Yagita, H and Yokoyama, T (2014). Renal atrophy after ischemia-reperfusion injury depends on massive tubular apoptosis induced by TNFα in the later phase. *Med Mol Morphol* **47**: 213–223.
9. Tse, MT (2013). Trial watch: sepsis study failure highlights need for trial design rethink. *Nat Rev Drug Discov* **12**: 334.
10. Bernard, GR, Francois, B, Mira, JP, Vincent, JL, Dellinger, RP, Russell, JA *et al.* (2014). Evaluating the efficacy and safety of two doses of the polyclonal anti-tumor necrosis factor-α fragment antibody AZD9773 in adult patients with severe sepsis and/or septic shock: randomized, double-blind, placebo-controlled phase IIb study*. *Crit Care Med* **42**: 504–511.
11. He, L and Hannon, GJ (2004). MicroRNAs: small RNAs with a big role in gene regulation. *Nat Rev Genet* **5**: 522–531.
12. Elbashir, SM, Harborth, J, Lendeckel, W, Yalcin, A, Weber, K and Tuschl, T (2001). Duplexes of 21-nucleotide RNAs mediate RNA interference in cultured mammalian cells. *Nature* **411**: 494–498.
13. Brower, V (2010). RNA interference advances to early-stage clinical trials. *J Natl Cancer Inst* **102**: 1459–1461.
14. Nguyen, QD, Schachar, RA, Nduaka, CI, Sperling, M, Klamerus, KJ, Chi-Burris, K *et al.*; MONET Clinical Study Group. (2012). Evaluation of the siRNA PF-04523655 versus ranibizumab for the treatment of neovascular age-related macular degeneration (MONET Study). *Ophthalmology* **119**: 1867–1873.
15. Nguyen, QD, Schachar, RA, Nduaka, CI, Sperling, M, Basile, AS, Klamerus, KJ *et al.*; DEGAS Clinical Study Group. (2012). Dose-ranging evaluation of intravitreal siRNA PF-04523655 for diabetic macular edema (the DEGAS study). *Invest Ophthalmol Vis Sci* **53**: 7666–7674.
16. Kanasty, RL, Whitehead, KA, Vegas, AJ and Anderson, DG (2012). Action and reaction: the biological response to siRNA and its delivery vehicles. *Mol Ther* **20**: 513–524.
17. Zhang, Y, Satterlee, A and Huang, L (2012). *In vivo* gene delivery by nonviral vectors: overcoming hurdles? *Mol Ther* **20**: 1298–1304.
18. Sirsi, SR and Borden, MA (2012). Advances in ultrasound mediated gene therapy using microbubble contrast agents. *Theranostics* **2**: 1208–1222.
19. Qin, S, Caskey, CF and Ferrara, KW (2009). Ultrasound contrast microbubbles in imaging and therapy: physical principles and engineering. *Phys Med Biol* **54**: R27–R57.
20. Lan, HY, Mu, W, Tomita, N, Huang, XR, Li, JH, Zhu, HJ *et al.* (2003). Inhibition of renal fibrosis by gene transfer of inducible Smad7 using ultrasound-microbubble system in rat UUO model. *J Am Soc Nephrol* **14**: 1535–1548.
21. Li, F, Jin, L, Wang, H, Wei, F, Bai, M, Shi, Q *et al.* (2014). The dual effect of ultrasound-targeted microbubble destruction in mediating recombinant adeno-associated virus delivery in renal cell carcinoma: transfection enhancement and tumor inhibition. *J Gene Med* **16**: 28–39.
22. Inoue, H, Arai, Y, Kishida, T, Shin-Ya, M, Terauchi, R, Nakagawa, S *et al.* (2014). Sonoporation-mediated transduction of siRNA ameliorated experimental arthritis using 3 MHz pulsed ultrasound. *Ultrasonics* **54**: 874–881.
23. Kurosaki, T, Kawakami, S, Higuchi, Y, Suzuki, R, Maruyama, K, Sasaki, H *et al.* (2014). Kidney-selective gene transfection using anionic bubble lipopolyplexes with renal ultrasound irradiation in mice. *Nanomedicine* **10**: 1829–1838.
24. Li, DJ, Tang, Q, Shen, FM, Su, DF, Duan, JL and Xi, T (2009). Overexpressed alpha7 nicotinic acetylcholine receptor inhibited proinflammatory cytokine release in NIH3T3 cells. *J Biosci Bioeng* **108**: 85–91.
25. Yin, H, Kanasty, RL, Eltoukhy, AA, Vegas, AJ, Dorkin, JR and Anderson, DG (2014). Non-viral vectors for gene-based therapy. *Nat Rev Genet* **15**: 541–555.
26. Stokman, G, Qin, Y, Rácz, Z, Hamar, P and Price, LS (2010). Application of siRNA in targeting protein expression in kidney disease. *Adv Drug Deliv Rev* **62**: 1378–1389.
27. Takabatake, Y, Isaka, Y, Mizui, M, Kawachi, H, Shimizu, F, Ito, T *et al.* (2005). Exploring RNA interference as a therapeutic strategy for renal disease. *Gene Ther* **12**: 965–973.
28. Shimizu, H, Hori, Y, Kaname, S, Yamada, K, Nishiyama, N, Matsumoto, S *et al.* (2010). siRNA-based therapy ameliorates glomerulonephritis. *J Am Soc Nephrol* **21**: 622–633.
29. Hamar, P, Song, E, Kökény, G, Chen, A, Ouyang, N and Lieberman, J (2004). Small interfering RNA targeting Fas protects mice against renal ischemia-reperfusion injury. *Proc Natl Acad Sci USA* **101**: 14883–14888.

30. Höcherl, K, Schmidt, C, Kurt, B and Bucher, M (2010). Inhibition of NF-kappaB ameliorates sepsis-induced downregulation of aquaporin-2/V2 receptor expression and acute renal failure *in vivo*. *Am J Physiol Renal Physiol* **298**: F196–F204.
31. Ma, D, Lim, T, Xu, J, Tang, H, Wan, Y, Zhao, H *et al.* (2009). Xenon preconditioning protects against renal ischemic-reperfusion injury via HIF-1alpha activation. *J Am Soc Nephrol* **20**: 713–720.
32. Hauser, PV, Pippin, JW, Kaiser, C, Krofft, RD, Brinkkoetter, PT, Hudkins, KL *et al.* (2010). Novel siRNA delivery system to target podocytes *in vivo*. *PLoS One* **5**: e9463.
33. Wan, C, Allen, TM and Cullis, PR (2014). Lipid nanoparticle delivery systems for siRNA-based therapeutics. *Drug Deliv Transl Res* **4**: 74–83.
34. Liu, Y, Miyoshi, H and Nakamura, M (2006). Encapsulated ultrasound microbubbles: therapeutic application in drug/gene delivery. *J Control Release* **114**: 89–99.
35. Lieberthal, W and Nigam, SK (1998). Acute renal failure. I. Relative importance of proximal vs. distal tubular injury. *Am J Physiol* **275**: F623–F631.
36. Zuckerman, JE, Choi, CH, Han, H and Davis, ME (2012). Polycation-siRNA nanoparticles can disassemble at the kidney glomerular basement membrane. *Proc Natl Acad Sci USA* **109**: 3137–3142.
37. Bartlett, DW, Su, H, Hildebrandt, IJ, Weber, WA and Davis, ME (2007). Impact of tumor-specific targeting on the biodistribution and efficacy of siRNA nanoparticles measured by multimodality *in vivo* imaging. *Proc Natl Acad Sci USA* **104**: 15549–15554.
38. Russo, LM, Sandoval, RM, McKee, M, Osicka, TM, Collins, AB, Brown, D *et al.* (2007). The normal kidney filters nephrotic levels of albumin retrieved by proximal tubule cells: retrieval is disrupted in nephrotic states. *Kidney Int* **71**: 504–513.
39. Ichimura, T, Bonventre, JV, Bailly, V, Wei, H, Hession, CA, Cate, RL *et al.* (1998). Kidney injury molecule-1 (KIM-1), a putative epithelial cell adhesion molecule containing a novel immunoglobulin domain, is up-regulated in renal cells after injury. *J Biol Chem* **273**: 4135–4142.
40. Mishra, J, Ma, Q, Prada, A, Mitsnefes, M, Zahedi, K, Yang, J *et al.* (2003). Identification of neutrophil gelatinase-associated lipocalin as a novel early urinary biomarker for ischemic renal injury. *J Am Soc Nephrol* **14**: 2534–2543.
41. Iseki, K, Iseki, C, Ikemiya, Y and Fukiyama, K (1996). Risk of developing end-stage renal disease in a cohort of mass screening. *Kidney Int* **49**: 800–805.
42. Tsunoda, S, Mazda, O, Oda, Y, Iida, Y, Akabame, S, Kishida, T *et al.* (2005). Sonoporation using microbubble BR14 promotes pDNA/siRNA transduction to murine heart. *Biochem Biophys Res Commun* **336**: 118–127.
43. Un, K, Kawakami, S, Yoshida, M, Higuchi, Y, Suzuki, R, Maruyama, K *et al.* (2012). Efficient suppression of murine intracellular adhesion molecule-1 using ultrasound-responsive and mannose-modified lipoplexes inhibits acute hepatic inflammation. *Hepatology* **56**: 259–269.
44. Misseri, R, Meldrum, DR, Dinarello, CA, Dagher, P, Hile, KL, Rink, RC *et al.* (2005). TNF-alpha mediates obstruction-induced renal tubular cell apoptosis and proapoptotic signaling. *Am J Physiol Renal Physiol* **288**: F406–F411.
45. Ramesh, G and Reeves, WB (2002). TNF-alpha mediates chemokine and cytokine expression and renal injury in cisplatin nephrotoxicity. *J Clin Invest* **110**: 835–842.
46. Al-Lamki, RS, Wang, J, Vandenabeele, P, Bradley, JA, Thiru, S, Luo, D *et al.* (2005). TNFR1- and TNFR2-mediated signaling pathways in human kidney are cell type-specific and differentially contribute to renal injury. *FASEB J* **19**: 1637–1645.
47. Ko, GJ, Jang, HR, Huang, Y, Womer, KL, Liu, M, Higbee, E *et al.* (2011). Blocking Fas ligand on leukocytes attenuates kidney ischemia-reperfusion injury. *J Am Soc Nephrol* **22**: 732–742.
48. Hotta, K, Sho, M, Yamato, I, Shimada, K, Harada, H, Akahori, T *et al.* (2011). Direct targeting of fibroblast growth factor-inducible 14 protein protects against renal ischemia reperfusion injury. *Kidney Int* **79**: 179–188.
49. Adachi, T, Sugiyama, N, Gondai, T, Yagita, H and Yokoyama, T (2013). Blockade of death ligand TRAIL inhibits renal ischemia reperfusion injury. *Acta Histochem Cytochem* **46**: 161–170.
50. Castaneda, MP, Swiatecka-Urban, A, Mitsnefes, MM, Feuerstein, D, Kaskel, FJ, Tellis, V *et al.* (2003). Activation of mitochondrial apoptotic pathways in human renal allografts after ischemiareperfusion injury. *Transplantation* **76**: 50–54.
51. Gobé, G, Zhang, XJ, Cuttle, L, Pat, B, Willgoss, D, Hancock, J *et al.* (1999). Bcl-2 genes and growth factors in the pathology of ischaemic acute renal failure. *Immunol Cell Biol* **77**: 279–286.
52. Rabb, H, Ramirez, G, Saba, SR, Reynolds, D, Xu, J, Flavell, R *et al.* (1996). Renal ischemic-reperfusion injury in L-selectin-deficient mice. *Am J Physiol* **271**: F408–F413.
53. Kelly, KJ, Williams, WW Jr, Colvin, RB, Meehan, SM, Springer, TA, Gutierrez-Ramos, JC *et al.* (1996). Intercellular adhesion molecule-1-deficient mice are protected against ischemic renal injury. *J Clin Invest* **97**: 1056–1063.
54. Li, L and Okusa, MD (2010). Macrophages, dendritic cells, and kidney ischemia-reperfusion injury. *Semin Nephrol* **30**: 268–277.
55. Linfert, D, Chowdhry, T and Rabb, H (2009). Lymphocytes and ischemia-reperfusion injury. *Transplant Rev (Orlando)* **23**: 1–10.
56. Bolisetty, S and Agarwal, A (2009). Neutrophils in acute kidney injury: not neutral any more. *Kidney Int* **75**: 674–676.
57. Lindner, JR, Song, J, Xu, F, Klibanov, AL, Singbartl, K, Ley, K *et al.* (2000). Noninvasive ultrasound imaging of inflammation using microbubbles targeted to activated leukocytes. *Circulation* **102**: 2745–2750.
58. Bayfield, MS, Lindner, JR, Kaul, S, Ismail, S, Sheil, ML, Goodman, NC *et al.* (1997). Deoxygenated blood minimizes adherence of sonicated albumin microbubbles during cardioplegic arrest and after blood reperfusion: experimental and clinical observations with myocardial contrast echocardiography. *J Thorac Cardiovasc Surg* **113**: 1100–1108.
59. Hadjantonakis, AK, Gertsenstein, M, Ikawa, M, Okabe, M and Nagy, A (1998). Generating green fluorescent mice by germline transmission of green fluorescent ES cells. *Mech Dev* **76**: 79–90.
60. Kami, D, Kitani, T, Kishida, T, Mazda, O, Toyoda, M, Tomitaka, A *et al.* (2014). Pleiotropic functions of magnetic nanoparticles for *ex vivo* gene transfer. *Nanomedicine* **10**: 1165–1174.